PHYSICAL REVIEW B VOLUME 13, NUMBER 4 15 FEBRUARY 1976

Level quantization and broadening for band electrons in a magnetic field: Magneto-optics throughout the band

W. Y. Hsu† and L. M. Falicov
Department of Physics,‡ University of California, Berkeley, California 94720
(Received 16 July 1975)

The problem of the electronic structure of a perfect tight-binding crystal under a constant magnetic field is studied. Quantitative analysis based on a method of continuous fractions is developed. This method is compatible with the magnetic translation group. Calculations are carried out for various fields and an interpolation scheme, valid for fields up to 10^6 G, is presented. In the two directions perpendicular to the field, the density of electronic states consists of subbands—i.e., broadened levels—separated by gaps. The broadening is negligible for most levels. It is, however, paramount in narrow energy ranges close to two-dimensional saddle points, where for all practical purposes, the subbands merge into a single continuum. The resulting electronic structure is applied to study the magneto-optical response of a hypothetical simple-cubic crystal with an infinitely narrow core state. Wavelength and field modulations are discussed; excitonic effects are not included.

I. INTRODUCTION

The energy spectrum of an electron in the simultaneous presence of an external magnetic field $\vec{H}$ and a periodic crystal potential $V(\vec{r})$ constitutes a difficult and by now classical problem. It is difficult because the effects of the potential $V(\vec{r})$ and the field $\vec{H}$ are quite different in nature. The former causes the formation of energy bands while the latter quantizes the electronic motion and tends to form narrow levels. The problem is further complicated by the fact that the two natural "periods," introduced by the field H and the potential $V(\vec{r})$, respectively, are, for most values of the field, incommensurable.

In general, for $\vec{H}$ along a symmetry—or any rational index—direction $\hat{z}$, the motion of the electron along $\hat{z}$ is unaffected by the field $\vec{H}$ and decouples completely from the remaining two directions. This is why $\hbar k_3$, the z component of the crystal momentum, remains a good quantum number. The magnetic field, however, does affect the transverse electronic motion (i.e., motion in the x-y plane). In free space, the electronic levels for the transverse motion are discrete and equivalent to those of a hypothetical harmonic oscillator with cyclotron frequency as its resonant frequency.[1] Physically, these allowed levels, the so-called Landau levels, consist of only those cyclotron orbits enclosing an integral number of magnetic flux quanta. In fact, this is the cornerstone of Onsager's semiclassical approach[2] to the problem of band electrons in a magnetic field. In short, cyclotron orbits compatible to the zero-field energy band, rather than the free-space circular ones, are used in this method. The Onsager quantization scheme[2,3] thus partially takes into account effects of the periodic potential. Broadening effects, the other important consequence of the crystal potential, are however totally neglected in this approximation. Onsager's approach, nonetheless, yields accurate results whenever applied to situations where the energy of the transverse motion is almost a maximum or a minimum. That is, the transverse energy is in the vicinity of two-dimensional (2D) critical points T_0 (minimum) or T_2 (maximum). Therefore, the energy levels around three-dimensional (3D) Van Hove singularities M_0 (minimum) and M_3 (maximum), regardless of the direction of the applied field H, are well understood. On the other hand, the semiclassical method breaks down completely near 2D saddle points T_1. There the broadening effect is paramount. Hence, electronic behavior around 3D saddle points M_1 and M_2 is more complicated. When the magnetic field is in the direction of that principal axis along which the effective mass has a different sign, i.e., when the 2D singularity is either T_0 or T_2, Onsager's scheme can still be applied. But, if the field is along any of the other two principal axes, i.e., the 2D singularity is of the T_1 type, broadening effects must be taken into proper account.

Experimentally, Landau levels just about M_0 points can be observed by magneto-optical transitions.[4] These transitions have been studied thoroughly for almost 20 years. Similar transitions at saddle points M_1, however, were observed only recently.[5] In this case, the understanding of the phenomenon is not quite complete. The magneto-optical behavior above M_1 points was first discussed theoretically by Bassani *et al.*[6,7] Their analysis is incomplete because of their assumed quadratic energy band. Obviously, a quadratic expansion is valid only in the immediate vicinity in k space of one given M_1 saddle point. Therefore, contributions from the rest of the band, including points of the same energy and other degen-

erate M_1 points, have not been taken into account. In order to treat the complete structure more realistically, a better band picture has to be used. We study, in this paper, the case of a magnetic field along one of the cubic axes of a simple-cubic crystal with an infinitely narrow core state and a single s-like tight-binding conduction band. In our geometry, it is obvious that the situation studied by Bassani *et al.*[6,7] corresponds only to the case of the M_1 saddle point along the z axis, where the quantization of almost-circular orbits perpendicular to z is still valid. The peaks above the M_1 critical point in the magneto-optical absorption discussed by them are then due to these quantized transverse-electron orbits. As far as the topological properties in the transverse plane are concerned, such a point actually corresponds to a 2D minimum (T_0). It is also obvious that electrons with very small k_3 components, which move close to the other two M_1 singularities, can also contribute to the optical absorption. However, for electrons in such orbits, the crystal potential broadening cannot be neglected. We thus have to investigate in detail the broadening of Landau levels in a solid.

Physically, this broadening is related to the periodicity in the reciprocal space, i.e., a typical solid-state effect. Harper[8] first demonstrated that the broadening is extremely small and negligible near the top (T_2) and bottom (T_0) of the 2D bulk band—i.e., the band for constant k_3. This corresponds to the case studied by Bassani *et al.*[6,7] In these regions, the center of gravity of each level is just that given by the semiclassical Onsager scheme. Harper also found that the broadening effect is much more prominent near the center of the 2D band; this is the case that we want to study now. Yet, owing to the breakdown of his WKB approximation, Harper was unable to calculate the width of the levels there. Nor was he able to show quantitatively where and when the broadening effect becomes important. Independently, Zil'berman[9] employed essentially the method of linear combination of atomic orbitals to the study of the same phenomenon. However, his calculated electronic levels do not even agree with the semiclassical ones in the appropriate limit. The disagreement occurs in zeroth order and hence cannot be attributed to the higher-order corrections discussed by Roth.[10] The discrepancy actually stems from his assumptions and approximations which are, unfortunately, not all true. Since then, many other calculations have been undertaken by different authors.[11–14] All of them, however, are for the extremely-high-field limit, typically for fields larger than 10^6 G. For all practical purposes, they are all beyond the range of present experimental interest. In Sec. II, we study the problem of level broadening based on a method of continued fractions. An interpolation formula is found numerically and applied to determine when the broadening effect is important for magnetic fields in the range of 0.1 to 10 kG. A simplified but realistic working model is then proposed. In Sec. III, we apply the model developed in Sec. II to the study of magneto-optical transitions. The absorption coefficient and its modulation spectra are calculated. The modulation spectra are those with respect to the frequency of the radiation field and to the strength of the applied magnetic field. Our calculations and discussions are given in Sec. IV.

II. THEORY OF LEVEL QUANTIZATION AND BROADENING

A. Difference equation

According to the tight-binding model, the electronic band structure of an s band in a simple-cubic lattice, in the absence of a magnetic field, is given by the following expression:

$$E(\vec{k}) = -E_1(\cos k_1 a + \cos k_2 a + \cos k_3 a), \tag{2.1}$$

with

$$\vec{k} = (k_1, k_2, k_3), \tag{2.2}$$

where a is the lattice constant and E_1 is the nearest-neighbor energy-transfer integral. The properties of this band structure are very well known. It extends from $-3E_1$ to $3E_1$ in energy and has a total bandwidth of $6E_1$. The standard 3D Van Hove singularities M_0, M_1, M_2, and M_3 are found at energies of $-3E_1$, $-E_1$, E_1, and $3E_1$, respectively. In any plane normal to one of the cubic axes, say $\hat{z}$, the corresponding 2D band has a total width of $4E_1$. It ranges from $-3E_1$ to E_1 in energy in the $k_3 = 0$ plane; from $-E_1$ to $3E_1$ at the top of the zone, i.e., $k_3 = \pi/a$; and from $-2E_1$ to $2E_1$ in a plane midway between the center and top of the zone, i.e., $k_3 = \pi/2a$. At the center of each 2D band, there is a logarithmic T_1 singularity. This is one of the standard 2D Van Hove critical points. In principle, each 3D Van Hove singularity can be obtained by combining the 2D density of states with the appropriate 1D density of states (from the $\hat{z}$ direction). For example, critical points M_1 arise from the T_1 singularity of the 2D band in the $k_3 = 0$ plane together with the L_0 singularity, i.e., the minimum of the 1D band from the $\hat{z}$ direction (contributions from $k_1 = \pi/a$, $k_2 = k_3 = 0$ and from $k_2 = \pi/a$, $k_1 = k_3 = 0$), as well as from the T_0 singularity in the 2D band in the $k_3 = \pm\pi/a$ plane together with the L_1 (maximum) singularity of the 1D ($\hat{z}$ direction) band ($k_1 = k_2 = 0$, $k_3 = \pm\pi/a$).

If we neglect interband transitions, and the Zeeman effect, the Schrödinger equation describing the behavior of a bulk electron in the presence of a magnetic field $\vec{H}$ is given by

$$E(\vec{\kappa})U(\vec{r}) = WU(\vec{r}). \tag{2.3}$$

In the above equation, the Hamiltonian $E(\vec{\kappa})$ is obtained from Eq. (2.1) with $\vec{\kappa}$, a differential operator, defined by

$$\vec{\kappa} = -i\vec{\nabla} + \frac{|e|}{\hbar c}\vec{A}(\vec{r}). \tag{2.4}$$

This is the well-known effective-mass theory of Luttinger and Kohn.[15] In Eqs. (2.3) and (2.4), the position vector $\vec{r}$ is

$$\vec{r} = (r_1, r_2, r_3), \tag{2.5}$$

and W is the energy eigenvalue limited to the range $-3E_1$ to $3E_1$. For the case of a uniform magnetic field along $\hat{z}$, one of the cubic axes, $\vec{A}(\vec{r})$ takes on the simple form

$$\vec{A}(\vec{r}) = (0, Hr_1, 0). \tag{2.6}$$

With this gauge, k_2 and k_3 are both good quantum numbers.

We can now apply the method of separation of variables with the following choice of wave function:

$$U(\vec{r}) = f(r_1)\ e^{i(k_2 r_2 + k_3 r_3)}. \tag{2.7}$$

Substitution of (2.7) into (2.3) yields

$$f(r_1 + a) + f(r_1 - a) + 2\left[\frac{W}{E_1} + \cos k_3 a + \cos\left(\frac{|e|Ha}{\hbar c} r_1 + k_2 a\right)\right] f(r_1) = 0. \tag{2.8}$$

This is a difference equation which can be cast into a more familiar form by a simple change of variable,

$$r_1 = na. \tag{2.9}$$

Thus, we obtain

$$f(n+1) + f(n-1) - 2q(n) f(n) = 0, \tag{2.10}$$

with

$$q(n) = -\left[W/E_1 + \cos k_3 a + \cos(n\epsilon^2 + k_2 a)\right]. \tag{2.11}$$

The dimensionless quantity ϵ^2 appearing above is defined as

$$\epsilon^2 = |e| Ha^2/\hbar c. \tag{2.12}$$

It is simply the magnetic flux through a unit cell measured in terms of $\hbar c/|e|$. Equation (2.10) is known as Harper's equation.[8] Further reduction into a symmetric form, given below in (2.17) and (2.18), can easily be achieved if we take the following steps[9]:

(i) Fourier transformation

$$F(y) = \sum_{n=-\infty}^{\infty} f(n)\ e^{iny}. \tag{2.13}$$

(ii) Definition of a new function Ψ,

$$\Psi(y) = F(y)\ e^{ik_2 ay/\epsilon^2}. \tag{2.14}$$

(iii) Change of variable (simple scaling)

$$x = y/\epsilon. \tag{2.15}$$

(iv) Definition of the differential operator p,

$$p = i\frac{\partial}{\partial x}. \tag{2.16}$$

The effective Schrödinger equation so obtained is

$$\mathcal{H}_{eff}\Psi(x) = \lambda\Psi(x), \tag{2.17}$$

with

$$\mathcal{H}_{eff} = \cos\epsilon p + \cos\epsilon x \tag{2.18}$$

and

$$\lambda = -\tfrac{1}{2}(W/E_1 + \cos k_3 a). \tag{2.19}$$

As usual,[9] the operator $\cos\epsilon p$ is defined by

$$\cos\epsilon p\ \Psi(x) \equiv \tfrac{1}{2}\left[\Psi(x+\epsilon) + \Psi(x-\epsilon)\right]. \tag{2.20}$$

What we have done so far is just to separate the longitudinal motion, which is unaffected by the magnetic field, from the transverse one. The 1D Schrödinger equation given in (2.17) and (2.18) then describes the electronic motion in any plane normal to the field. The reduced energy eigenvalue λ, which is defined in a dimensionless form according to (2.19), has values between -1 and 1. It is important to emphasize that the longitudinal motion, even though it is separated from the transverse one, is being fully taken into account by the reduced eigenvalue λ. We have not made, within the one-band approximation, any expansion or any other approximation.

Equation (2.17) can now be studied by standard methods of band-structure theory. In the present consideration, we are only interested in the width of each subband and the energy gap between two adjacent levels, but not the detailed dispersion relation within a given subband. Thus we can simplify our calculation considerably by choosing proper expansion wavefunctions.[16] The method that we employ (see the Appendix) is a simple extension of the analysis commonly used in the study of Mathieu functions.[17] It is also equivalent to the Feenberg method of continued fractions,[18] as well as compatible with the theory of magnetic groups.[14,19]

B. Calculation and analysis

We calculate the energy subbands from Eqs. (2.17) and (2.18) by the method of continued fractions developed in the Appendix. For a magnetic field $H \sim 10$ kG and a lattice constant $a \sim 2.5$ Å, ϵ^2 is of the order of 10^{-4} and hence $N \equiv 2\pi/\epsilon^2$, defined by Eq. (A4) of the Appendix, is very much larger than 1. Naturally, the polynomials obtained in the Appendix, such as (A14), cannot be solved analytically. Instead, numerical methods have to be used. In the present calculation, as explained in the Appendix, we consider cases of integer N only.

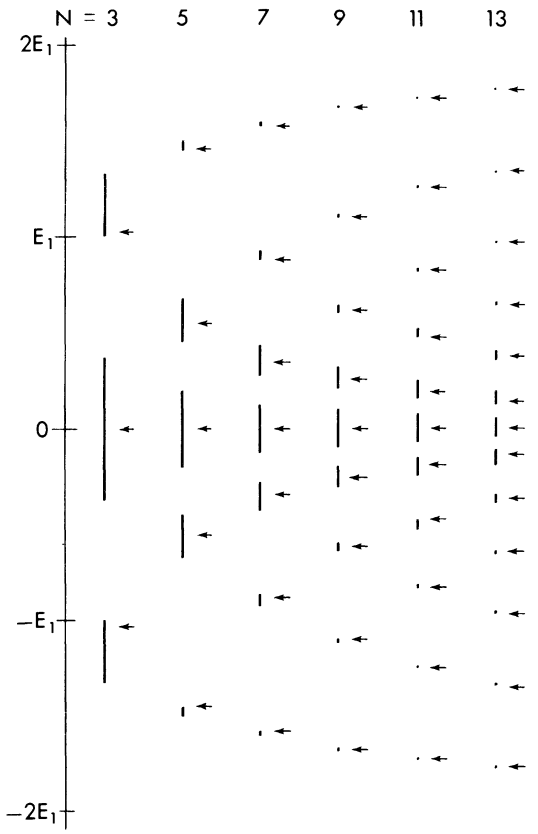

FIG. 1. Subbands (vertical lines) as calculated by the method of continued fractions versus the discrete Onsager levels (horizontal arrows).

Our results for a few cases of relatively small N, i.e., extremely large magnetic fields, are reported in Fig. 1. For comparison, on the same graph, energy levels as calculated from the Onsager quantization rules[2,3] are plotted side by side. It is obvious that the broadening effect is indeed small near the top and bottom of the 2D bulk band. On the other hand, it is very large near the center. It is also obvious that Roth's correction[10] to the Onsager quantization is quite important here. However, for larger values of N, the correction is in general very small. In the range of experimental interest such corrections can be neglected altogether. Our results are similar to those obtained by other authors.[11-14] It is also worth mentioning that each subband contains the same number of states. This number depends only on the applied field H.

Let us call those orbits with negative eigenvalues λ electron orbits and those with positive λ hole orbits. The energy of the lth hole subband at its center of gravity is denoted as E_l ($E_l > 0$). Because of the electron-hole symmetry, the lth electron subband is characterized by the energy $-E_l$. The index l goes between 0 and $N/2-1$ or $(N-1)/2$; its origins are at the bottom (electrons) and at the top (holes) of the 2D band and the maximum values are achieved close to the middle (T_1 singularity) of the band. In addition, for both types of orbits, we define Δ_l as the width of the lth subband and Γ_{l-1} as the gap between the top of the $(l-1)$th and the bottom of the lth subbands. The energy-gap-to-width ratio R_l for the lth level (either electron or hole) is

$$R_l = \Gamma_{l-1}/\Delta_l. \tag{2.21}$$

Whence large R_l ($R_l \gg 1$) indicates isolated discrete levels. On the other hand, $R_l \sim 1$ corresponds to subbands that are somewhat widened and closer to each other. Finally, a very small R_l ($R_l \ll 1$) implies that the well-broadened levels are so close that essentially they have merged, for all practical purposes, into a single continuum. To simplify the description, in the following we will use the terms "discrete" and "continuum" in a qualitative manner. They are to be understood, respectively, as a narrow subband and a collection of wide subbands separated by vanishingly small gaps.

In general, for each fixed value of N or, for that matter, the magnetic field H [cf. definitions (2.12) and (A4)], we obtain the empirical result

$$R_l = e^{-B+A/l}, \tag{2.22}$$

whenever l is large. In (2.22), both A and B are functions of N but are independent of l. Typical behavior is shown in Fig. 2. If A and B are plotted as a function of N on a log-log scale, two straight lines with slopes equal to 2 and 1, respectively, are discovered (Fig. 3). We thus obtain the interpolation formula

$$R_l = e^{-\mu N+\nu N^2/l}. \tag{2.23}$$

In the above equation, μ and ν are two numerical constants given by

$$\mu = 0.6962 \tag{2.24}$$

and

$$\nu = 0.3438. \tag{2.25}$$

Analytic calculations can be carried out in the semiclassical regions. It is easy to show that there R_l obeys an equation similar to (2.23). Notice that R_l is nonanalytic in the limit of zero magnetic field.

The 2D densities of states for differend applied fields H can now be calculated easily. For the range that we are considering, i.e., 0.1 to 10 kG, practically all of them look the same and some of them are given in Fig. 4. Beyond doubt, the electronic levels are being converted into a continuum at the center of the band. We have in fact just

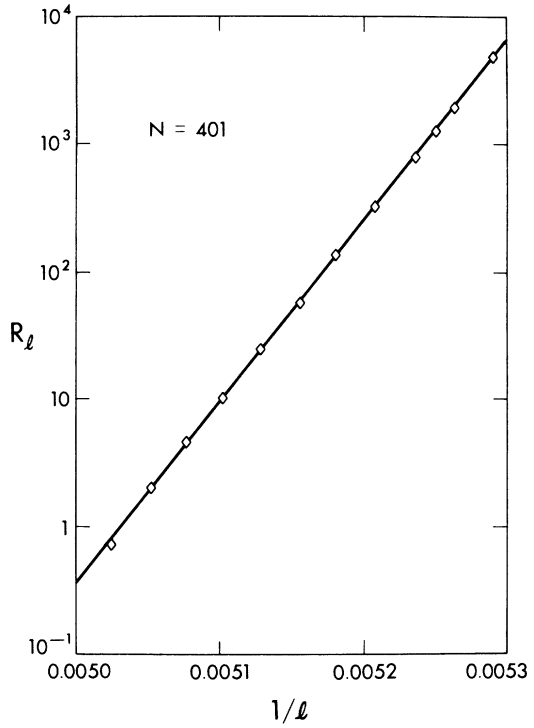

FIG. 2. Typical behavior of the band-gap–to–width ratio R_l for the lth subband as a function of l^{-1}.

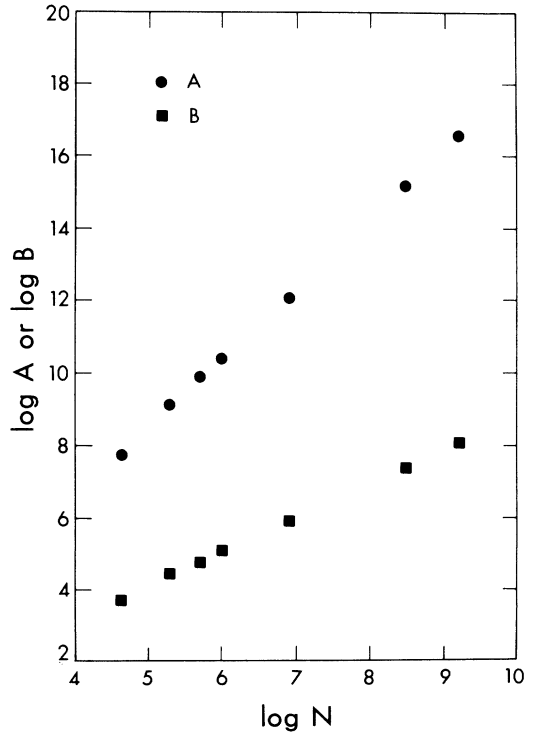

FIG. 3. Behavior of the slope A and the intercept B as functions of $N = (2\pi\hbar c/|e|Ha^2)$.

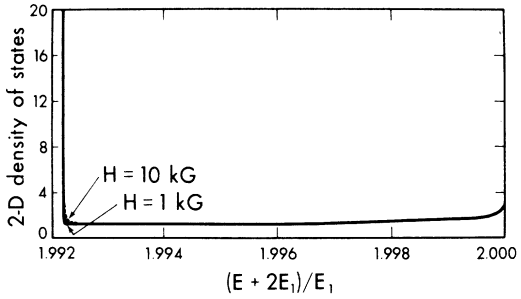

FIG. 4. Two-dimensional density-of-states plots in a transverse plane (i.e., a plane normal to the magnetic field). The horizontal axis is energy, measured from the bottom of the 2D band in units of E_1. Only that portion from $1.992E_1$ to $2E_1$ in energy is shown. The 2D density of states is nonzero from 0 to $4E_1$ and is symmetric with respect to $2E_1$. The transition from discrete narrow Landau levels into a quasicontinuum near the center takes place at $1.9922E_1$. Notice the transition is very sharp and almost field independent for the cases that we have calculated. The logarithmic singularity at $2E_1$ is also visible.

demonstrated how the solid-state broadening can reconcile the well-established existence of discrete levels near the band edges (T_0 and T_2) but, at the same time, the equally conspicuous absence of any quantization near the center (T_1). Notice also how sharp the transition from discrete levels to the continuum is, typically within only a few levels. Similar, almost abrupt, transitions from very narrow to much wider bands are also observed in the behavior of Mathieu functions.[20] In the present case, the very sharp transition is directly related to the logarithmic T_1 singularity at the center of the 2D band in the transverse plane. Physically it simply means that a large number of states around the center of the 2D band participate coherently in the broadening process. They are essentially free to wander from one well in reciprocal space to another. The other important consequence of Eqs. (2.23)–(2.25) is the magnetic-field-independent nature of the transition for the fields we have calculated. For this range, the transition always takes place at an energy $0.0078E_1$ from the center of the 2D band.[21] This is, some 99.6% of the band is occupied by discrete levels. Only about 0.4% is in a continuum. The number of subbands participating in this continuum is about 6×10^4 for a magnetic field of 0.1 kG and 6×10^2 for 10 kG. The 3D density of states, in the presence of a magnetic field, can be understood by superposition of suitable 2D ones as explained previously. The quasicontinuum discussed above then leads to the usual $(E_c - E)^{1/2}$ behavior below M_1 critical points. It does not lead to any new structure above M_1. However, owing to the small ex-

tent of this strip of quasicontinuous states, it is important to take into proper consideration those discrete Landau levels just beyond the strip. Taking everything into consideration, we conclude that nearly two-thirds of the 3D band, namely, from $-3E_1$ to $-1.0078E_1$ and from $1.0078E_1$ to $3E_1$, is with discrete 2D levels. About 0.25% of the band, from $-1.0078E_1$ to $-E_1$ and from E_1 to $1.0078E_1$, is continuous. The remaining section, i.e., from $-E_1$ to E_1, is a superposition of noninteracting discrete 2D levels and a continuum. In particular, in the range from $-0.9922E_1$ to $0.9922E_1$, complicated beat patterns due to the simultaneous presence of both electron and hole orbits are observable. Meanwhile, such beat patterns disappear in the range from $-E_1$ to $-0.9922E_1$ and also from $0.9922E_1$ to E_1.

C. Step-function model

We have concluded that the broadening effect is very small for most of the 2D band except near the center. There, the effect of broadening completely overwhelms that of the field-induced quantization. The level width is such that essentially there is a continuum. In other words, level quantization has been almost completely suppressed. The electrons behave just as if there were no applied magnetic field. Physically, this is due to the very large electron tunneling from one well in the reciprocal space to another, as given by (2.17) and (2.18). This is actually the quantum-mechanical version of the very same singular orbit associated semiclassically with the 2D Van Hove critical point T_1. Similar behavior should take place for crystals with other lattice geometries. It is, however, possible to have directions away from high-symmetry directions, where closed but very extended semiclassical orbits exist. In this case, the level quantization produces discrete but very densely packed levels, and the broadening should be studied there separately. The broadening, as in our example, is due to the probability of tunneling between adjacent orbits.

In order to simplify the analysis of the magneto-optical absorption of a simple-cubic crystal, we develop a step-function approximation here. In the energy range

$$2E_1 > |E| > bE_1, \tag{2.26}$$

where for the present calculation b is 0.0078, we assume the levels to be completely discrete and given by the simpler but accurate Onsager quantization. That is, as a first approximation, we neglect broadening effects in this region where they are very small. In reality, the small but finite level broadening causes a change in the line shape of the absorption spectrum. This is then separately discussed for a typical absorption peak. We further neglect the small energy interval in which the transition from levels to continuum actually takes place. Instead, it is assumed that the transition occurs at, and is completed within, one level (hence, the name step-function model). Beyond such a level, i.e., for

$$|E| \leq bE_1, \tag{2.27}$$

the electronic levels are those given by the zero-field continuum. Of course, all phenomena due to the transition region will be lost under our approximation. In principle, they can be studied by using a gradual approximation, e.g., an exponential cutoff, instead of the present abrupt step approximation. However, we have not carried out such a calculation here as we are convinced that it will only provide a small quantitative but not any qualitative correction.

III. MAGNETO-OPTICAL PROPERTIES

A. Absorption coefficient

For the sake of definiteness, we assume here that the crystal has a narrow valence band. In the absence of a magnetic field, we can approximate the valence band by

$$\epsilon_v(\vec{k}) = -E_v. \tag{3.1}$$

The conduction band $\epsilon_c(\vec{k})$ is given by (2.1). The positive constants E_v and E_1 are such that

$$E_v > 3E_1 > 0. \tag{3.2}$$

This last condition guarantees a conduction band of energy higher than the valence band. In the presence of an external magnetic field along one of the cubic axes, the valence band remains unchanged but the conduction band is now subjected to the effects of both quantization and broadening. Following the analysis given in Sec. II, we have

$$\epsilon_c(\vec{k}, H) = \begin{cases} -E_1 \cos k_3 a - E_l, & -2E_1 \leq -E_l < -bE_1, \\ -E_1 \cos k_3 a + w, & -bE_1 \leq w \leq bE_1, \\ -E_1 \cos k_3 a + E_l, & bE_1 < E_l \leq 2E_1, \end{cases} \tag{3.3}$$

where

$$w = -E_1(\cos k_1 a + \cos k_2 a). \tag{3.4}$$

For each integer l, the positive quantity E_l is the solution of the integral equation

$$\int_{E_l/(2E_1)}^{1} K'(z)\,dz = \tfrac{1}{4}\pi\epsilon^2(l+\tfrac{1}{2}), \tag{3.5}$$

where ϵ^2 is proportional to the magnetic field H as defined in (2.12) and K' is the associated complete elliptic integral of the first kind.[22]

The optical absorption coefficient α is proportional to the matrix element of the electric dipole moment. As usual, within the tight-binding ap-

proximation, this matrix element is a constant. The absorption coefficient α is also proportional to the joint density of states J defined by

$$J(\omega,H)=\sum_{\vec{k}}\delta(\hbar\omega+\epsilon_v(\vec{k},H)-\epsilon_c(\vec{k},H)). \tag{3.6}$$

In (3.6), $\delta(x)$ is the Dirac δ function and ω is the frequency of the radiation field. For the present case, $\epsilon_v(\vec{k},H)$ is a mere constant and only causes a shift of the energy scale. As a consequence, J is equivalent to the 3D density of states of the conduction band. As we have commented before, the density of states can be written as the convolution of the 1D density of states along the field direction and the 2D density of states $\mathfrak{D}_2$ in a plane normal to it. In functional form, this relationship is

$$J(\omega,H)=\frac{1}{\pi}\int_{-E_1}^{E_1}dz\,(E_1^2-z^2)^{-1/2}\mathfrak{D}_2(\hbar\omega-E_v+z), \tag{3.7}$$

with

$$z=E_1\cos k_3a. \tag{3.8}$$

In the absence of an external magnetic field H, it is easy to show that

$$\mathfrak{D}_2(\hbar\omega-E_v+z)=\frac{1}{\pi^2E_1}K'\left(\frac{\hbar\omega-E_v+z}{2E_1}\right), \tag{3.9}$$

and in the presence of a field H,

$$\mathfrak{D}_2(\hbar\omega-E_v+z)=\begin{cases}\dfrac{\epsilon^2}{2\pi}\displaystyle\sum_l\delta(\hbar\omega-E_v+z+E_l), & -2E_1<-E_l<-bE_1,\\[2ex] \dfrac{1}{\pi^2E_1}K'\left(\dfrac{\hbar\omega-E_v+z}{2E_1}\right), & -bE_1\le\hbar\omega-E_v+z\le bE_1,\\[2ex] \dfrac{\epsilon^2}{2\pi}\displaystyle\sum_l\delta(\hbar\omega-E_v+z-E_l), & bE_1<E_l<2E_1,\\[2ex] 0 & \text{otherwise.}\end{cases} \tag{3.10}$$

Finally, we have the following expression for the absorption coefficient[23]:

$$\alpha(\omega,H)=(C/\omega)J(\omega,H). \tag{3.11}$$

In the preceding equation, C is a constant independent of both ω and H. Except for the weighting factor ω^{-1}, the absorption spectrum measures the density of states of the conduction band.

For the sake of clarity, we only report below the absorption coefficient for two different cases. Similar expressions for other frequency and magnetic field ranges can be obtained quite easily and are not reported here.

(i) In the absence of a magnetic field and if

$$-3E_1\le\hbar\omega-E_v\le-E_1, \tag{3.12}$$

it is straightforward to show that

$$\alpha=\frac{C}{\pi^3E_1\omega}\int_{-2-\eta}^{1}d\xi\,(1-\xi^2)^{-1/2}K'\left(\frac{\eta+\xi}{2}\right), \tag{3.13}$$

where

$$\eta=(\hbar\omega-E_v)/E_1 \tag{3.14}$$

and

$$\xi=z/E_1=\cos k_3a. \tag{3.15}$$

(ii) In the presence of a field H, and in the region

$$-E_1+bE_1\le\hbar\omega-E_v\le E_1-bE_1, \tag{3.16}$$

it can be shown that α now consists of three terms,

$$\alpha=\alpha_1+\alpha_2+\alpha_3, \tag{3.17}$$

where α_1 arises from the quantized electron orbits, α_3 from the hole orbits, and α_2 from the continuum. They are respectively given by

$$\alpha_1=\frac{C\epsilon^2}{2\pi^2E_1\omega}\sum_{l=l_1}^{l_2}\left[1-\left(\frac{E_l}{E_1}+\eta\right)^2\right]^{-1/2}, \tag{3.18}$$

$$\alpha_2=\frac{C}{\pi^3E_1\omega}\int_{2-b+\eta}^{2+b+\eta}d\xi\,(1-\xi^2)^{-1/2}K'\left(\frac{\eta+\xi}{2}\right), \tag{3.19}$$

and

$$\alpha_3=\frac{C\epsilon^2}{2\pi^2E_1\omega}\sum_{l=l_3}^{l_4}\left[1-\left(\frac{E_l}{E_1}-\eta\right)^2\right]^{-1/2}. \tag{3.20}$$

In (3.18) and (3.20), the integers l_1–l_4 are separately determined by

$$-E_{l_1-1}<\hbar\omega-E_v-E_1<E_{l_1}, \tag{3.21}$$

$$-E_{l_2}<-bE_1<-E_{l_2+1}, \tag{3.22}$$

$$E_{l_3}<\hbar\omega-E_v+E_1<E_{l_3-1}, \tag{3.23}$$

and

$$E_{l_4+1}<bE_1<E_{l_4}. \tag{3.24}$$

Because of conditions (3.21) and (3.23), each term in the series (3.18) and (3.20) is real. In other frequency ranges, one or two of the three terms in Eq. (3.17) may be missing. Consequently, patterns of quite different shape are observed for different regions. Some of them are shown in Fig. 5.

Let us describe below the over-all character-

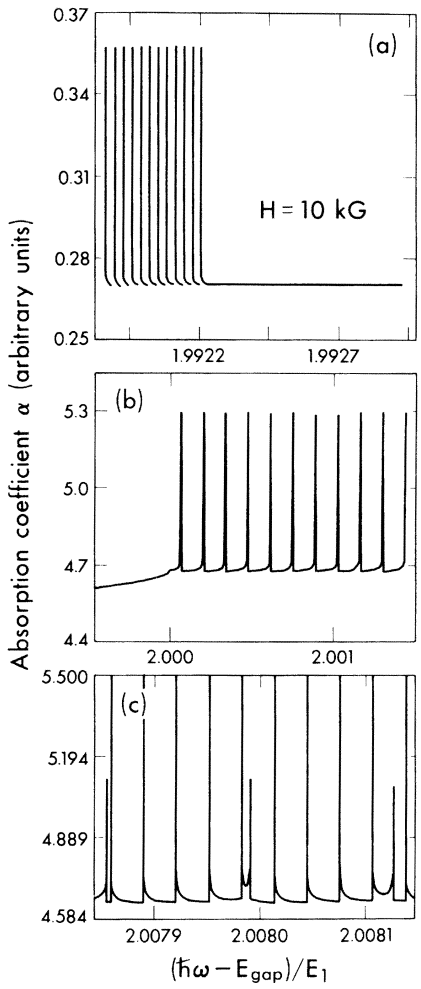

FIG. 5. Absorption coefficient: (a) at the transition from 2D discrete levels into a quasicontinuum; (b) at critical points M_1; and (c) at the onset of beat patterns. In all three cases the energy is measured from the bottom of the conduction band in units of E_1. The energy gap between the conduction and valence bands is denoted by E_{gap} and is equal to $(E_v - 3E_1)$.

istics of the absorption coefficient α. It is obvious that α vanishes identically [cf. Eq. (3.10)] whenever

$$|\hbar\omega - E_v| > 3E_1. \tag{3.25}$$

The factor ω^{-1} is smooth and without structure in the range of interest. Thus, all singularities (or peaks) in the absorption spectra have to come from the joint density of states J. Consequently, the zero-field absorption coefficient, as a function of the variable $\hbar\omega - E_v$, is smooth except for discontinuities in the derivative at the Van Hove critical points M_0, M_1, M_2, and M_3 of the joint density of states. In the presence of a field, the absorption coefficient behaves in a very different manner. Peaks, more precisely, singularities, which are a consequence of the quantization effects of the applied field, appear almost everywhere. However, effects of the solid-state broadening over those of the quantization restore the system to the zero-field behavior in the ranges

$$-(E_1 + bE_1) \leq \hbar\omega - E_v \leq -E_1 \tag{3.26}$$

and

$$E_1 \leq \hbar\omega - E_v \leq E_1 + bE_1. \tag{3.27}$$

In particular, the absorption coefficient α exhibits no peak whatsoever in these two regions. The only singularities are the relatively mild one-sided square-root-type at M_1 and M_2, respectively. In the present calculation, the extent of each of these regions, equal to bE_1, is insensitive to the value of the applied field H. On the other hand, singularities, similar to those discussed by Bassani *et al.*,[6] are found just above M_1,

$$-E_1 \leq \hbar\omega - E_v \leq -(E_1 - bE_1), \tag{3.28}$$

and just below M_2,

$$E_1 - bE_1 \leq \hbar\omega - E_v \leq E_1. \tag{3.29}$$

Typical behavior is shown in Fig. 5(b). Behavior in the regions

$$-3E_1 < \hbar\omega - E_v < -(E_1 + bE_1) \tag{3.30}$$

and

$$E_1 + bE_1 < (\hbar\omega - E_v) < 3E_1 \tag{3.31}$$

is well known. Singularities in the former region are from electron orbits, while the latter regions consist of peaks from hole orbits. The behavior just above the M_0 threshold can be found in the literature[7] and hence is not reproduced here. On the other hand, the behavior near the transition from 2D discrete subbands into a quasicontinuum has not been reported before. Typical behavior is shown in Fig. 5(a). In the middle energy range, i.e.,

$$-(E_1 - bE_1) \leq \hbar\omega - E_v \leq E_1 - bE_1, \tag{3.32}$$

both electron and hole subbands as well as the continuum contribute. The formulas given in Eqs. (3.17)–(3.20) are precisely for this range. The absorption curve around the lower limit of the range (3.32) is reported in Fig. 5(c). Owing to the presence of both electronlike and holelike resonances, the pattern is quite complicated. Also notice how the line shapes differ for the two types of peaks. As $\hbar\omega - E_v$ moves towards the center, beat patterns can also be observed. This is due to the almost identical cyclotron frequencies for electrons and holes. We emphasize that the processes we are disucssing here are all one-photon transitions. By no means should they be confused with

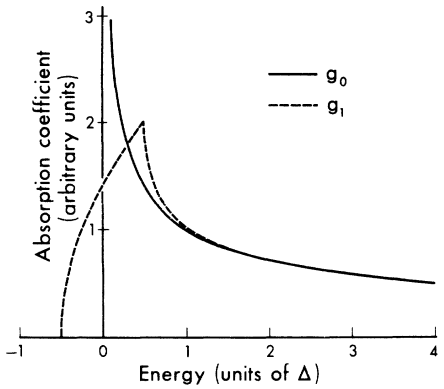

FIG. 6. Absorption line shapes: solid curve neglects the finite width of the narrow subband; dashed curve includes the width.

the two-photon processes discussed by Bassani *et al.*[7] If we filter out all the field-dependent singularities we recover the smooth background. As expected, it is just the zero-field continuum.

In order to investigate the change in the absorption line shape due to the small but finite width Δ of each subband, we replace in the 2D density of states (3.10) the previously used δ function by the following normalized square well:

$$f(x)=\begin{cases}1/\Delta, & -\Delta/2\le x\le\Delta/2\ ,\\ 0, & \text{otherwise}\ .\end{cases} \tag{3.33}$$

Now, instead of the simple line shape

$$g_0(x)=\begin{cases}0, & x<0\ ,\\ x^{-1/2}, & x>0\ ,\end{cases} \tag{3.34}$$

we have

$$g_1(x)=\begin{cases}0, & x<-\Delta/2\ ,\\ (2/\Delta)(x+\Delta/2)^{1/2}, & -\Delta/2<x<\Delta/2\\ (2/\Delta)[(x+\Delta/2)^{1/2}-(x-\Delta/2)^{1/2}], & x>\Delta/2.\end{cases} \tag{3.35}$$

They are plotted in Fig. 6. Of course, as Δ diminishes, $g_1(x)$ eventually goes over to $g_0(x)$. The sharp cusp appearing at $\Delta/2$ in $g_1(x)$ is due to the use of (3.33). Any other (smoother) function, such as a Gaussian or Lorentzian, will remove this cusp. The effects of these latter functions are well discussed[24,25] and will not be repeated here.

B. Modulated absorption spectra

We have also calculated two modulation spectra of the absorption coefficient α. They are the frequency- and magnetic-field-modulation spectra, respectively. Each of these is just the partial derivative of α with respect to the modulating parameter. The major advantage of differential spectroscopy is of course its much higher sensitivity.[24,25] Some of our numerically calculated spectra are shown in Figs. 7 and 8.

It is obvious that the quantization effects now manifest themselves as singularities of a stronger form: $(\omega-\omega_t)^{-3/2}$. Other new features are again consequences of the quantization-suppression mechanism discussed previously. Specifically, in the presence of a magnetic field, the singularities in the absorption coefficient α at M_1 and M_2 are

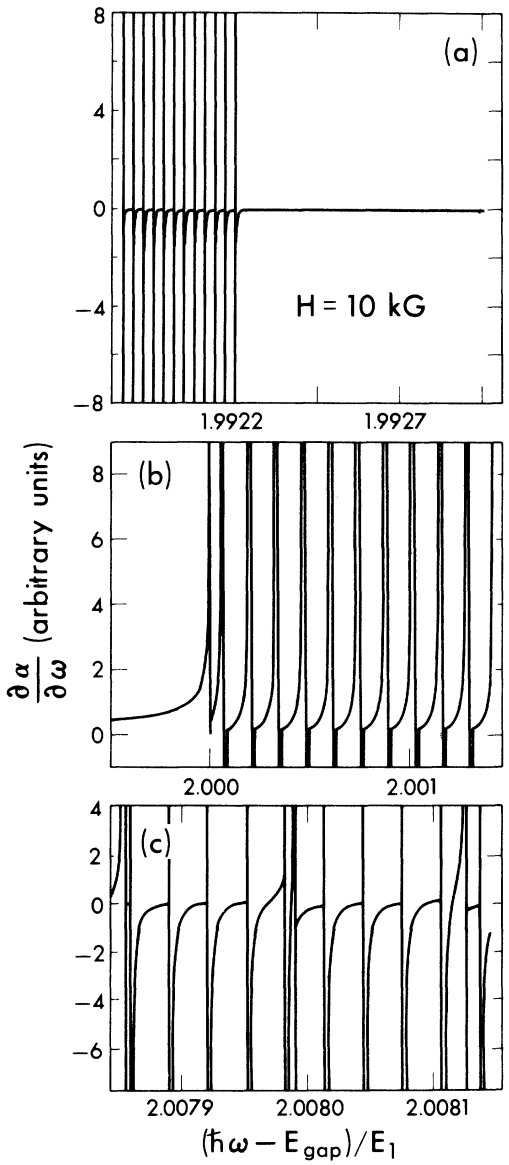

FIG. 7. Frequency-modulated absorption coefficient: (a) at the transition from 2D discrete levels into a quasicontinuum; (b) at critical points M_1; and (c) at the onset of beat patterns. In all three cases, the energy is measured from the bottom of the conduction band in units of E_1.

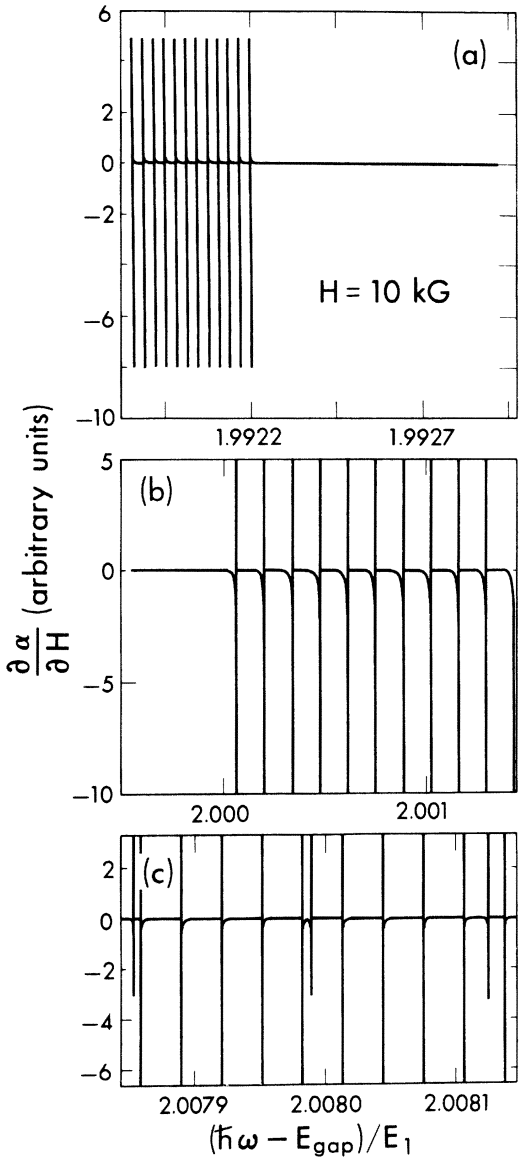

FIG. 8. Modulation spectrum with respect to the strength of the magnetic field: (a) at the transition from 2D discrete levels into a quasicontinuum; (b) at critical points M_1; and (c) at the onset of beat patterns. In all three cases, the energy is measured from the bottom of the conduction band in units of E_1.

susceptible only to the frequency variation but not at all to the magnetic field. Therefore, extra peaks occur at both M_1 and M_2 in the frequency modulation spectra but none whatsoever for the field-modulation spectra. Also notice the quite different line shapes for the hole- and electron-induced peaks in the two differential spectra as shown in Figs. 7(c) and 8(c).

As before, we have inspected the field-independent background of both spectra by filtering out all the field-induced peaks. The background for the frequency modulation is essentially similar to the appropriate zero-field one. On the other hand, the background for the magnetic field modulation is identically zero. This last phenomenon can be understood easily: The magnetic field only affects the relative positions of the field-induced peaks in the optical absorption spectra without changing the over-all background itself.

We have also applied Eq. (3.35) to the study of differential line shapes. For the case of frequency modulation, the proper line shape is

$$g_2(x) = \begin{cases} 0, & x < -\Delta/2\ , \\ (1/\Delta)(x+\Delta/2)^{-1/2}, & -\Delta/2 < x < \Delta/2\ , \\ (1/\Delta)[(x+\Delta/2)^{-1/2} - (x-\Delta/2)^{-1/2}], & \\ & x > \Delta/2. \end{cases} \tag{3.36}$$

As commented before, the discontinuities at $\pm\Delta/2$ are due to the square-well function (3.33) and can be removed easily. It is slightly more complicated for the case of magnetic field modulation. In general, both x $(=\hbar\omega - E_l)$ and the width Δ depend on the applied field H. However, in the semiclassical regime, the field dependence of E_l dominates that of the width. Thus, we obtain, in this limit

$$g_3(x) = -h_l\, g_2(x), \tag{3.37}$$

where the coefficient h_l depends only on the level number l and is independent of the field H. Thus g_3 is simply proportional to g_2.

IV. CONCLUSIONS AND DISCUSSION

We have developed in this paper a method based on continued fractions to study the electronic levels in the presence of a magnetic field. We find that the solid-state phenomenon of level broadening is ultimately responsible for transforming discrete Landau-like levels into a quasicontinuum. In general, the nature of a given level (i.e., whether it is discrete or part of a quasicontinuum) is determined by the competition of field-induced quantization and solid-state broadening. For a simple-cubic crystal with the magnetic field H along one of the cubic axes, the transition is found to be very sharp and essentially independent of the magnetic field H for the values that we have calculated. This leads to the suppression of field-induced peaks below M_1. We also show that frequency-modulation spectra are quite different from magnetic-field-modulation ones. First of all, their relative line shapes are quite different. Second, for the frequency modulation, a satellite peak, or a shoulder depending on the extent of excitonic broadening,[25–27] appears at M_1 and M_2 but none whatsoever for the magnetic field modulation.

The Coulomb attraction between electrons and holes from different bulk bands, the so-called excitonic effects,[26,27] has not been included in the

present consideration. The major effects are (i) to cause a shift as well as a broadening in the resonant peaks and (ii) to enhance further or suppress each individual peak.[5,26,28] As a result, quite different line shapes can occur.[5] Effects of a broad valence band can be taken into account by including suitable selection rules. The present formalism can also be applied to situations where the magnetic fields are not along an axis of high symmetry.

APPENDIX

In this appendix, the 1D effective Schrödinger equation (2.17)–(2.18) is studied by the method of continued fractions. This method is basically an extension of the one used in the analysis of Mathieu functions.[17]

We seek solutions of Eqs. (2.17) and (2.18) in the form of either

$$\Psi_{\text{even}}(x)=\sum_{l=0}^{\infty} A_{2l+s}\cos[\epsilon(l+s/2)x] \tag{A1}$$

or

$$\Psi_{\text{odd}}(x)=\sum_{l=0}^{\infty} B_{2l+s}\sin[\epsilon(l+s/2)x], \tag{A2}$$

and with

$$s=0,1. \tag{A3}$$

We further define the following quantities:

$$N=2\pi/\epsilon^2, \tag{A4}$$

$$V_l=2[\lambda-\cos(l\epsilon^2/2)]=2[\lambda-\cos(l\pi/N)], \tag{A5}$$

$$G_e(l)=A_l/A_{l-2}, \tag{A6}$$

and

$$G_o(l)=B_l/B_l/B_{(l-2)}. \tag{A7}$$

Substitution of either (A1) or (A2) into (2.17) and (2.18) and application of (A4)–(A7) yields four sets of recursion relations,

(i) Even $s=0$ case;

$$G_e(2)=V_0,$$
$$G_e(4)=V_2-[2/G_e(2)], \tag{A8}$$

and

$$G_e(l+2)=V_l-[1/G_e(l)].$$

(ii) Odd $s=0$ case:

$$G_o(4)=V_2$$

and

$$G_o(l+2)=V_l-[1/G_o(l)]. \tag{A9}$$

For both of the above cases, $l=4, 6, 8, 10, \ldots$.

(iii) Even $s=1$ case:

$$G_e(3)=V_1-1$$

and

$$G_e(l+2)=V_l-[1/G_e(l)]. \tag{A10}$$

(iv) Odd $s=1$ case:

$$G_o(3)=V_1+1$$

and

$$G_o(l+2)=V_l-[1/G_o(l)]. \tag{A11}$$

For cases (3) and (4), $l=3, 5, 7, 9, \ldots$.

Continued fractions can readily be deduced through Equations (A8)–(A11). For instance, Eq. (A8) yields the following:

$$\frac{2}{V_0}=V_2-\cfrac{1}{V_4-\cfrac{1}{V_6-\cfrac{1}{V_8-\ddots}}} \tag{A12}$$

For the case of integral values of N, N is closely related to the total number of subbands present in the system. Nonintegral rational values of N lead to the splitting of each Landau subband into clusters of subbands. Azbel proved under quite general conditions that the separation between these sub-subbands is small.[29] Numerical calculations confirm his proof.[14] For all practical purposes, we can instead consider the coarse-grained properties of all clusters derived from a single Landau level.[30] In reality, the fluctuation of the applied magnetic field as well as spatial inhomogeneity more than wipes out the tiny gaps among the sub-subbands. Thus, nature has performed the coarse-grained average for us already and the question of whether N is rational or irrational becomes, more or less, academic. Without loss of generality, we thus assume N to be an integer. It is now straightforward to show that

$$V_{l+2N}=V_l. \tag{A13}$$

In other words, the continued fractions are periodic and reducible to polynomials of finite orders. For example, Eq. (A12) is equivalent to

$$(\lambda-1)^{-1}=2(\lambda-\cos\epsilon^2)-\cfrac{1}{2(\lambda-\cos2\epsilon^2)-\cfrac{1}{\ddots-\cfrac{1}{2[\lambda-\cos(\lambda-1)\epsilon^2]-(\lambda-1)^{-1}}}}, \tag{A14}$$

where Eqs. (A5) and (A13) have been used. Hence, we are able to calculate the bandwidth, level separation, and the density of states quantitatively.

---

†IBM Predoctoral Fellow. Present address: Department of Physics, University of Illinois, Urbana, Ill. 61801.

‡Work supported in part by The National Science Foundation through Grant No. DMR72-03106-A01.

[1]L. Landau, Z. Phys. 54, 629 (1930).

[2]L. Onsager, Philos. Mag. 43, 1006 (1952).

[3]See also, L. M. Falicov, in *Electrons in Crystalline Solids* (I.A.E.A., Vienna, 1973), p. 207.

[4]See, for instance, the review article by B. Lax and J. G. Mavroides, in *Semiconductors and Semimetals*, edited by R. K. Willardson and A. C. Beer (Academic, New York, 1967), Vol. 3, p. 321.

[5]S. O. Sari, Phys. Rev. Lett. 26, 1167 (1971); Phys. Rev. B 6, 2304 (1972); Solid State Commun. 12, 705 (1973); Phys. Rev. Lett. 30, 1323 (1973).

[6]A. Baldereschi and F. Bassani, Phys. Rev. Lett. 19, 66 (1967).

[7]F. Bassani and A. Baldereschi, Surf. Sci. 37, 304 (1973).

[8]P. G. Harper, Proc. Phys. Soc. Lond. A 68, 874 (1955).

[9]G. E. Zil'berman, Zh. Eksp. Teor. Fiz. 30, 1092 (1956) [Sov. Phys.-JETP 3, 835 (1957)].

[10]L. M. Roth, Phys. Rev. 145, 434 (1966).

[11]D. Langbein, Phys. Rev. 180, 633 (1969).

[12]W. G. Chambers, Phys. Rev. 140, A 135 (1965).

[13]H. W. Capel, Physica 54, 361 (1971).

[14]P. S. Kapo and E. Brown, Phys. Rev. B 7, 3429 (1973); F. A. Butler and E. Brown, Phys. Rev. 166, 630 (1968).

[15]J. M. Luttinger and W. Kohn, Phys. Rev. 97, 869 (1955); G. H. Wannier, Rev. Mod. Phys. 34, 645 (1962).

[16]See, for example, C. Kittel, *Introduction to Solid State Physics*, 4th ed. (Wiley, New York, 1971), Chap. 9.

[17]For a comprehensive review see U.S. Bureau of Standards, *Tables Relating to Mathieu Functions* (Columbia University, New York, 1951), p. xv.

[18]P. M. Morse and H. Feshbach, *Methods of Theoretical Physics* (McGraw-Hill, New York, 1953), Vol. II, Chap. 9.

[19]J. Zak, Phys. Rev. 134, A1602 (1964); 134, A1607 (1964).

[20]J. C. Slater, Phys. Rev. 87, 807 (1952).

[21]The transition from discrete to continuum structure at $0.0078E_1$ from the center of the 2D band is a function of the dispersion relation (2.1), but surprisingly enough, not a function of magnetic field.

[22]See, for example, I. S. Gradshteyn and I. M. Ryzhik, *Table of Integrals, Series and Products*, translated by A. Jeffrey (Academic, New York, 1965), Chap. 8.

[23]L. M. Roth, B. Lax, and S. Zwerdling, Phys. Rev. 114, 90 (1959).

[24]R. L. Aggarwal, in *Semiconductors and Semimetals*, edited by R. K. Willardson and A. C. Beer (Academic, New York, 1972), Vol. 9, p. 151.

[25]M. Cardona, *Modulation Spectroscopy* (Academic, New York, 1969).

[26]R. J. Elliott, Phys. Rev. 108, 1384 (1957).

[27]J. O. Dimmock, in *Semiconductors and Semimetals*, edited by R. K. Willardson and A. C. Beer (Academic, New York, 1967), Vol. 3, p. 259; R. S. Knox, *Theory of Excitons* (Academic, New York, 1963).

[28]B. Velický and J. Sak, Phys. Status Solidi 16, 147 (1966).

[29]M. Ya. Azbel, Zh. Eksp. Teor. Fiz. 46, 929 (1964) [Sov. Phys.-JETP 19, 634 (1964)].

[30]E. Brown, Phys. Rev. 133, A1038 (1964).